

Adaptive DTOGI control algorithm for seamless grid integration and power quality enhancement in PMSG-based variable speed wind energy supply system

Devang B Parmar*, Ashutosh K Giri**

*(Ph.D Scholar, Gujarat Technological University, Ahmedabad-382424, Gujarat, India)

** (Government Engineering College Bharuch-392002, Gujarat, India)

ABSTRACT

This study presents effective operation for grid synchronization and enhanced power quality in a permanent-magnet synchronous generator (PMSG)-constructed variable-speed wind energy supply framework. When coupling two AC systems (PMSG and grid), independent control becomes challenging, resulting in instability of the DC-link voltage under diverse wind and load conditions. To address this issue, the proposed approach employs vector control on the PMSG side for precise speed regulation and rotor angle estimation through a reference quadrature current control loop, thereby ensuring optimal power extraction and seamless operation. A dual third-order generalized integrator phase-locked loop (DTOGI) control method is applied on the grid side to stabilize the DC link voltage and improve power quality by efficiently reducing harmonics and addressing grid disturbances. The coordinated control of both sides ensures stable system performance, reliable grid synchronization, and improved power quality under dynamic operating conditions. The results from the simulation confirmed the accomplishment of the proposed control strategy, showcasing improved stability and observance to grid standards.

Keywords - Permanent Magnet Synchronous Generator, Nonlinear load, Synchronization, Vector Control, Power quality.

Date of Submission: 10-05-2025

Date of acceptance: 21-05-2025

I. INTRODUCTION

The rapid growth in wind energy is driven by environmental benefits. However, the high cost associated with large and heavy generators remains a challenge. This review emphasizes the need to optimize PMSGs to enhance their cost-effectiveness and efficiency[1]. It examines multi-objective optimization strategies, mathematical modelling and validation methodologies, including the Finite Element Method (FEM), highlighting the positive impact of these innovations on the renewable energy sector. Recent control strategies for PMSG-based variable-speed wind turbines, focusing on power extraction and inverter control. It highlights advancements and challenges and provides valuable insights for improving the system efficiency and performance [2]. Hybrid adaptive virtual inertia control strategy uses fuzzy logic to enhance the frequency support in low inertia microgrids with renewable energy sources. This approach integrates kinetic-energy-based virtual inertia with virtual capacitance control to adjust control gains, thereby

ensuring frequency stability amidst disturbances and load variations [3]. This manuscript presents a sensorless nonlinear control approach for a PMSG in a wind energy system, employing Integral Sliding Mode Control (ISMC) alongside backstepping control methodologies. By employing a High-Gain Observer, it is possible to estimate torque and speed without the use of sensors, which in turn optimizes power extraction and enhances the quality of the grid. Simulations have demonstrated superior performance under various wind conditions and system uncertainties [4]. This paper provides a comprehensive review of wind energy conversion systems, with a particular emphasis on their aerodynamic, electrical, and mechanical components, as well as control strategies. It examines the principal findings, current research endeavours, and prospective advancements in wind energy technology [5]. This study examines WECS, focusing on generators, power converters, and grid-connection challenges, highlighting trends and power quality issues. It also explores the potential of

brushless doubly fed reluctance generators (BDFRG) [6]. This study examined offshore wind energy systems, compared device types, analysed challenges, and explored future trends for improved efficiency and control [7]. This study reviews advanced control strategies for WECS, highlights effective techniques for pitch angle, MPPT, and machine-side and grid-side controllers, and identifies the most efficient methods for improving the performance [8]. This study investigated a WECS using a PMSG connected to a grid. To enhance performance during grid faults, the control strategy integrates MPPT and pitch control, maximizing power generation while maintaining output voltage stability. Simulation results confirm the effectiveness of this approach [9]. This study presents an innovative rectifier design for variable-speed, high-power PMSG-based WECSs, incorporating with uncontrol rectifier. The operation and control methodologies of the rectifier are comprehensively detailed and validated through both simulations and experimental testing [10]. Study examined the use of an FOC with a PMSG to improve the energy capture and maintain control stability. The robustness was tested by varying the generator parameters, and simulations in MATLAB/Simulink were used to assess the system performance [11].

The results showed that the implemented control strategies for the PMSG-based wind energy system successfully ensured a stable performance under fluctuating wind conditions and grid faults. The optimized PI controller settings contribute to efficient energy conversion and maintain grid stability [12]. This study reviews DPGS structures using fuel cells and solar and wind power, discusses GSC control, harmonic compensation, and grid fault handling, and examines synchronization methods for effective control [13]. The modern control strategy enhances GSC performance under abnormal conditions by compensating for negative-sequence currents and using DSOGI-SPLL. It outperforms traditional methods in maintaining the stability and power quality [14]. An Improved PLL for high-voltage flexible power systems to enhance synchronization under harsh grid conditions. It addresses the limitations of traditional PLLs by integrating a repetitive control model for harmonic suppression and introducing DC bias elimination

and frequency adaptation. Simulations and experiments have confirmed this improved performance [15].

This study presents the development of a five-level multilevel inverter integrated with a photovoltaic (PV) array, aimed at enhancing power quality through the utilization of a shunt active power filter. Modified PLL addressed grid distortions. Simulations show improved performance and grid current THD within the IEEE-1547 standards [16]. DSOGI-PLL incorporating in-loop filtering was implemented in a three-phase solar grid system operating under irregular grid and load conditions. It extracts fundamental components that are free from DC offsets and harmonics, thereby maintaining a balanced grid current. Positive sequence voltages aid in accurate phase calculations. Simulations and tests confirmed IEEE-519 compliance [17]. This paper presents a Type-3 MNF-SOGI-PLL specifically developed for single-phase systems, which enhances the dynamic response and grid parameter estimation, while effectively rejecting the DC offset without phase delay. Experimental results confirmed its superior performance under different grid faults and disruptions [18]. This paper introduces an improved SOGI (ESOGI)-based PLL for single-phase grid synchronization, utilizing an all-pass filter to efficiently eliminate the DC offset. This approach improves the accuracy and reduces periodic ripples, with experimental results validating its performance [19]. This paper highlights an enhanced DSOGI-PLL for micro-grids to maintain synchronization under unbalanced voltages, harmonic pollution, and frequency fluctuations. By incorporating closed-loop feedback to eliminate harmonic components and utilizing zero-cross detection for an accurate frequency reference, the proposed method ensures a high-precision and robust dynamic performance [20]. This study addressed the limitations of the standard SRF-PLL in three-phase VSCs and proposed an alternative representation of advanced PLLs. This new approach simplifies integration into synchronous reference frame impedance models and enhances stability analysis [21]. This research emphasizes innovative PLLs that incorporate a steady-state linear Kalman filter for three-phase power systems. The analysis reveals that these PLLs are essentially identical to the existing SRF-PLL

structures and do not provide any performance advantages. This study explores various frequency-locked loops (FLLs) for single-phase grid applications, including standard SOGI-FLL and alternatives such as LKF-FLL, 1Φ-CBF-FLL, and CLO-FLL. It aims to address the lack of detailed analysis and comparison of these methods, highlighting their advantages and disadvantages [22].

1.1 The highlighted bullet points describe the contributions of the authors.

- The authors develop an effective generator-side control by utilizing a streamlined feedback loop to monitor rotor speed and position, converting dq to abc values. This approach enables independent control of the torque and field while minimizing generator resistive losses, ensuring maximum torque extraction with minimum current. The Hysteresis Current Controller provides precise switching pulses and maintains the performance under varying load conditions, wind speed fluctuations, and grid disturbances.
- A DTOGI-based control algorithm was applied on the grid side to generate a reference current for regulating the DC-link voltage in grid-connected systems. This control improves grid synchronization and optimizes the extraction of both fundamental and harmonic components from the grid current. This approach improves the dynamic response, robustness to grid disturbances, and phase estimation accuracy, making it particularly suitable for PMSG-based wind turbines.
- Additionally, the proposed controller improves power quality by maintaining stable DC-link voltage regulation, enabling efficient power transfer in both steady-state and dynamic conditions.
- The rest of this paper is structured as follows: The first section includes an introduction and a literature review, highlighting the benefits of the proposed control algorithm over other approaches. Section 2 details the configuration of the proposed system. The mathematical modelling of the control is predicated on these equations. A vector control approach was employed for generator-side control, whereas grid-side control utilized the

DTOGI Control Algorithm to generate the reference current. Section 3 presents various scenarios simulated using MATLAB Simulink, and Section 4 provides the conclusion of the paper.

II. SYSTEM DESCRIPTION

Figure 1 shows the control scheme of a grid-connected Wind-driven Permanent Magnet Synchronous Generator (W-PMSG) system, outlining its main components and control methods for efficient power conversion and integration with the grid. The Generator-Side Converter (GSC) plays a crucial role in converting the variable AC power generated by the PMSG into a stable DC output while ensuring optimal power extraction using Maximum Power Point Tracking (MPPT). The GSC employs hysteresis pulse-width modulation for precise current control, thereby ensuring a rapid wind dynamic response. It utilizes a dq control strategy, wherein the currents are transformed into a rotating reference frame to enable independent control of both active and reactive power. The d axis controls loop the DC link voltage, whereas the q axis current loop regulates the generator torque, facilitating efficient speed control and power optimization in accordance with wind speed variations.

The Grid-Side Converter (GSC) is responsible for converting regulated DC power into synchronized AC power that is compatible with grid standards. The system ensures sinusoidal

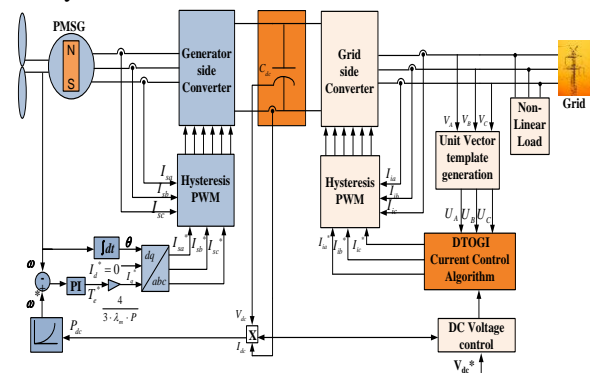


FIGURE1: Control Configuration for a Grid-Connected W-PMSG

current injection into the grid with minimal harmonic distortion, thereby preserving power quality. The GSC utilizes Hysteresis Pulse Width Modulation (PWM) for precise switching and DTOGI for accurate phase and frequency synchronization with the grid. Additionally, the GSC maintains a constant DC link voltage, ensuring seamless power flow between the generator side and the grid, even under variable wind and load conditions.

2.1 Generator-Side Closed Loop Converter Control
 The main intention is to operate a synchronous generator with a minimal current while maximizing the torque output. The PMSG-side closed-loop direct-axis reference current element should be modified to almost zero. The PMSG system generates most of its power from the integration of various wind speeds. To accurately support the PMSG power-speed curve, this technology typically exhibits a cubic relationship with the generator speed. The power-speed curve of the generator determines its speed reference, which is represented by the power next to the DC link. The reference torque be capable of be gained by comparing the reference speed to the actual speed and subsequently calculating the difference through the application of a proportional-integral regulator. Figure 2. illustrates a mathematical model of the closed-loop control technique.

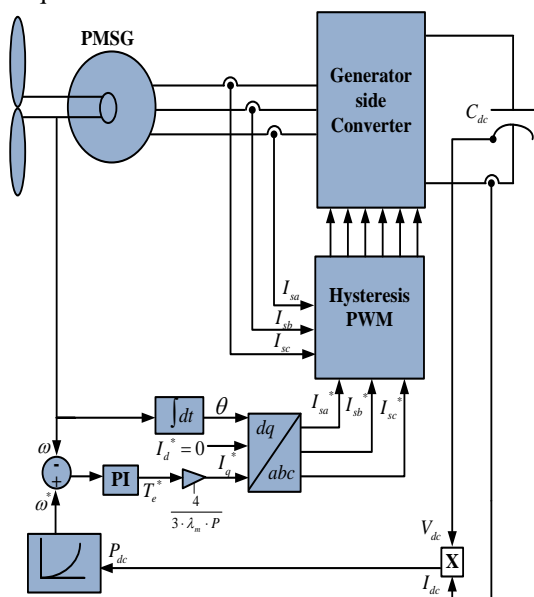


FIGURE 2: Generator-Side Vector Control Scheme. Power equation and the fundamental principle of

wind turbines as shown below,

$$P = \frac{1}{2} \rho C_p A V^3 \dots (1)$$

$$T_{turbine} = \frac{1}{2} \rho A C_p \frac{V}{\gamma} \dots (2)$$

The energy output of wind turbines is affected by the design of the turbine, the speed of the wind, and the prevailing weather conditions. Wind turbines operate optimally within a specific wind speed range and may cease operation or adjust their blade pitch to mitigate the damage from high-velocity winds. Wind turbines typically aggregate in wind farms to enhance their power-generation capacity. The cumulative turbine output of a wind farm constitutes the power production. Table 1 shows the influence of wind speed on various parameters associated with wind characteristics.

TABLE 1: Wind speed impacts different parameters

Wind Velocity (p.u)	MPPT Power (p.u.)	Generator Speed (p.u.)	Mechanical Torque (Nm)
1.04 (13 m/s)	0.7019 (2597 watt)	1.2 (95.83 r/s)	-43.10
0.96 (12 m/s)	0.5886 (2178 watt)	1.105 (88.26 r/s)	-36.81
0.88 (11 m/s)	0.4564 (1688 watt)	1.065 (85.02 r/s)	-28.74
0.8 (10 m/s)	0.3563 (1323 watt)	0.9879 (78.92 r/s)	-22.90
0.72 (9 m/s)	0.2788 (1031 watt)	0.899 (71.86 r/s)	-18.16
0.64 (8 m/s)	0.206 (762 watt)	0.8062 (64.39 r/s)	-14.10
0.56 (7 m/s)	0.1413 (522 watt)	0.7056 (56.36 r/s)	-10.79

The wind speed fluctuated between 10 m/s and 12 m/s. In an 8-pole PMSG control design, the generator rotational speed is 750 rpm, with an average wind speed of 10 m/s. The generator reached a maximum power output of 1.2 per unit (p.u.), decreasing to 0.7 p.u. below this speed. Figure 3 shows the turbine power profile.

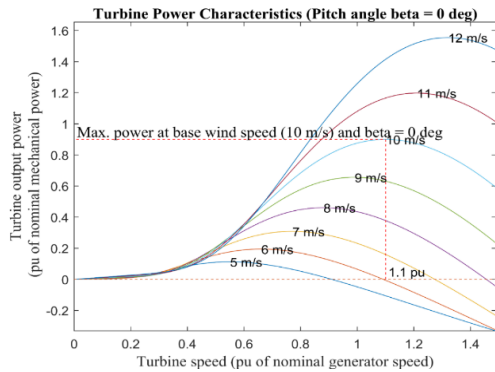


FIGURE 3: Power-speed Characteristics of the Wind Turbine.

The PMSG 3.7 kW wind turbine achieves peak power output at 0.9 p.u. maintaining this power until the wind speed reaches 10 m/s. To demonstrate the wind turbine power characteristics, the rotational speed was adjusted to 1.1 times the base generator speed. The pitch angle beta remained constant at zero. To represent the PMSG dynamic prototype in a rotating reference frame, the mathematical modelling formulas below were used.

$$V_q = L_q \frac{di_q}{dt} + R_s i_q - w_r \lambda_m + w_r L_d i_d \dots(3)$$

$$V_d = R_s i_d + L_d \frac{di_d}{dx} - w_r L_q i_q \dots(4)$$

Where R_s represents the stator resistance (in ohms), I_d & I_q are the d -axis and q -axis variables affecting the stator current (as measured in amps), λ_m (lambda) is the flux linkage (in Weber-turns), w_r (omega) is the rotor's angular velocity (radians per second) V_d and V_q are the stator voltage's d - and q -axis components, correspondingly (in volts).

To express the electromagnetic torque produced by the rotor, the following equation can be utilized:

$$T_e = \left(\frac{3}{2}\right) \left(\frac{P}{2}\right) [(L_d - L_q) i_q i_d - \lambda_m i_q] \dots(5)$$

When a cylindrical rotor is utilized, both L_d and L_q are reduced, transforming the equation into a suitable representation.

$$T_e = \left(\frac{3}{2}\right) \left(\frac{P}{2}\right) \lambda_m i_q \dots(6)$$

The significance of the quadrature axis reference-current element can be estimated using the following formula:

$$i_q^* = \frac{4}{3} \left(\frac{T_e^*}{P \lambda_m} \right) \dots(7)$$

These equations delineate the interaction between the electrical and mechanical components of a PMSG when it is represented in a reference frame that is in motion. To model and study the behaviour of the PMSG and integrate these equations over time, considering the starting conditions and external factors, such as load torque or wind speed, control methods can be used to change how the generator works to meet certain requirements, such as keeping the amount of electrical power produced steady or controlling the speed of the wind machine.

2.2 Grid side DTOGI Control Algorithm

This block diagram represents an advanced DTOGI algorithm designed for grid synchronization, particularly useful for systems like the 3.7 kW PMSG-based wind generation system. The input currents I_a, I_b, I_c are transformed from the three-phase abc reference frame to the stationary $\alpha\beta$ reference frame using the Clarke transformation. This remains crucial for simplifying the control system as it converts the sinusoidal waveforms into two orthogonal components (I_α and I_β).

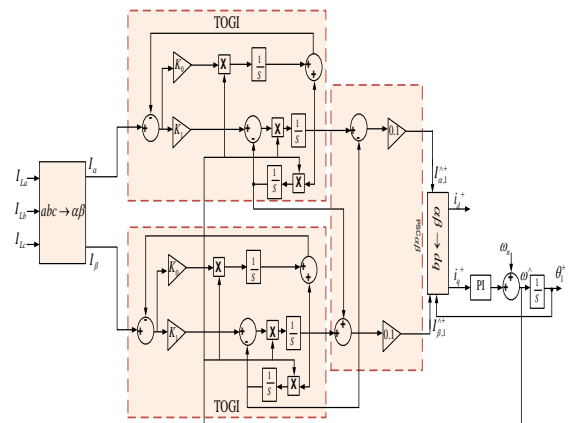


FIGURE 4: Block diagram of the DTOGI-based current-control algorithm.

The DTOGI structure generates orthogonal components, which are crucial for accurate frequency and phase detection, particularly under distorted grid conditions. Two TOGI blocks are

implemented to extract the fundamental frequency components from I_α and I_β . Each TOGI block consists of gain coefficients K_0 and K_1 to adjust the integrator dynamics. It is represented by integrator blocks to obtain the quadrature signals. Feedback loops to maintain oscillation at the fundamental frequency (Golestan et al., 2019).

The TOGI blocks the orthogonal output components, which are combined to Estimate the currents in the stationary reference frame. The transformation converts the positive sequence components from the stationary $\alpha\beta$ frame to the rotating frame dq . This transformation is necessary for decoupling the active and reactive power components, which facilitates better control in grid-tied applications.

This algorithm ensures accurate phase and frequency synchronization with the grid, which is crucial for seamless power injection. This enhances the robustness of the system against grid disturbances and harmonics, ensuring stable operation under variable wind speeds and grid conditions. The TOGI structure provides superior harmonic filtering compared with conventional PLLs, making it robust under distorted grid conditions (Golestan et al., 2021). The Feedback and integrators improve the PLL's dynamic response, therefore providing the rapid and precise tracking of grid fluctuations. Usually used for grid synchronizing in power systems, this block diagram shows a third-order generalized integrator phase-locked loop DTOGI. Three-phase currents are transformed via Clarke transformation into $\alpha\beta$ stationary components:

$$I_\alpha = I_a \quad \dots (8)$$

$$I_\beta = \frac{1}{\sqrt{3}}I_a + \frac{2}{\sqrt{3}}I_b \quad \dots(9)$$

From the stationary $\alpha\beta$ frame to the rotating dq frame, the positive sequence components are changed:

$$I_d^+ = I_\alpha^+ \cos(\theta^+) + I_\beta^+ \sin(\theta^+) \quad \dots (10)$$

$$I_q^+ = I_\alpha^+ \sin(\theta^+) + I_\beta^+ \cos(\theta^+) \quad \dots(11)$$

Decoupling the elements of active and reactive power depends on this change. Internal oscillator synchronization with grid frequency was accomplished using the PLL. It functions like this:

The quadrature component is used as the error signal.

$$e(t) = I_q^+ \quad \dots(12)$$

The error was processed using a PI controller as follows:

$$\omega_1 = K_p e(t) + K_i \int e(t) dt \quad \dots(13)$$

K_p and K_i are the proportional and integral gains.

The estimated frequency is then integrated to obtain the phase angle.

$$\theta^+ = \int \omega_1 dt \quad \dots(14)$$

This confirms phase angle θ^+ synchronisation with phase of the grid voltage. In summary, the $abc - \alpha\beta$ transformation simplifies the three-phase signals into two orthogonal components, making it easier to analyse and control in a stationary reference frame. TOGI then extracts the positive sequence components, providing effective harmonic rejection and improved signal quality. Using the $\alpha\beta - dq$ transformation, which decouples the active and reactive power components, these components are then transferred from the stationary $\alpha\beta$ frame to the rotating dq frame, therefore enabling exact control of power flow. Finally, the PLL synchronizes the internal phase angle with the grid voltage, thereby ensuring accurate frequency and phase tracking. This coordinated operation enhances grid stability and power quality, making the DTOGI highly effective for grid-connected renewable energy systems like the 3.7 kW PMSG-based wind generation system.

In the DTOGI control, the provided equation is intended to calculate a representative error or signal strength from various components. This value is then used by the proposed algorithm to adaptively reduce the mean square error, leading to optimal filter performance. Voltages at points of common coupling $(v_{sx})(v_{sy})(v_{sz})$ are recognized, and their magnitude is computed for DTOGI control application. The unit vectors in phase are calculated using Equation 16.

$$V_{Ar} = \sqrt{2 \left(\frac{v_{sx}^2 + v_{sy}^2 + v_{sz}^2}{3} \right)} \quad \dots(15)$$

$$u_{px} = \frac{v_{sx}}{V_{At}} \quad u_{py} = \frac{v_{sy}}{V_{At}} \quad u_{pz} = \frac{v_{sz}}{V_{At}} \quad ..(16)$$

$$u_{qx} = (u_{py} / \sqrt{3}) + (u_{pz} / \sqrt{3})$$

$$u_{qy} = (\sqrt{3}u_{px} / 2) + (u_{py} - u_{pz}) / (2\sqrt{3})$$

$$u_{qz} = (-\sqrt{3}u_{px} / 2) + (u_{py} - u_{pz}) / (2\sqrt{3}) \quad ..(17)$$

From the grid perspective, the voltage source inverter requires a minimum DC bus voltage that remains at least double the grid system's peak-phase voltage. The DC bus voltage was determined through a computational analysis. The DC capacitor value (C_{DC}) for the voltage source converter is provided below the equation.

$$V_{DC} = \frac{2\sqrt{2}V_{LL}}{\sqrt{3}} \quad(18)$$

III. SIMULATION RESULTS AND DISCUSSION

A closed-loop control system was developed and executed using MATLAB Simulink, and its dynamic performance was assessed under diverse operational situations. The results are shown in Figures 5–12. To facilitate comprehension of the system analysis, the findings were categorized into subsections based on the following structure:

3.1 Simulation result of Generator-side vector control

Figure 5 illustrates the dynamic response of a vector-controlled PMSG-based WECS to a step variation in wind speed. Initially, the wind speed remains at approximately 0.8 per unit (10 m/s) before increasing sharply to 0.95 per unit (12 m/s) around 0.85 seconds and then returns to 0.8 per unit at 1.15 seconds.

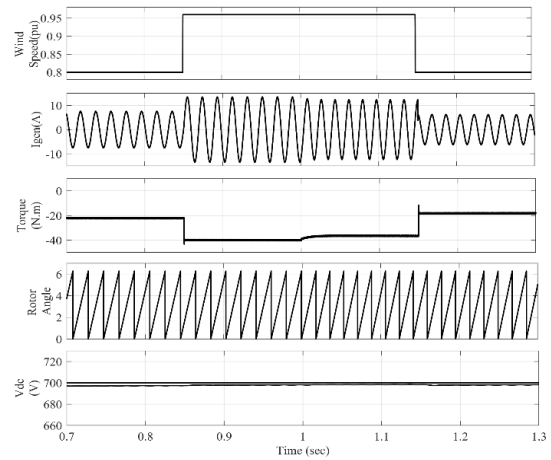


FIGURE 5 Simulation outcome of generator side vector control.

This sudden change affected the generator current, which exhibited a sinusoidal waveform with an increased amplitude corresponding to higher wind speed. A noticeable transient occurs during the transition, but the system quickly stabilizes owing to the proposed control strategy, which ensures precise regulation of the generator's electromagnetic torque and flux.

The generator torque, initially approximately (-20 Nm), drops to (-40 Nm) once the wind speed rises, reflecting the increased mechanical input from the turbine. As the wind speed returned to its initial value, the torque increased to (-20 Nm), demonstrating a clear relationship between the wind input and electromagnetic torque. The rotor angle plot shows a continuously increasing trend, indicating a steady rotation of the generator, with slight variations in the slope corresponding to wind speed changes. Meanwhile, the DC link voltage remained relatively stable at approximately 700V, with only minor fluctuations, suggesting an effective power regulation system. The use of vector control allows the standalone control of the torque and flux components of the generator, ensuring smooth operation and optimal power extraction under varying wind conditions. Overall, the waveform confirms that this control method responds efficiently to wind speed variations and maintains a stable operation with a well-regulated generator and power electronics.

Figure 6 illustrates the speed tracking performance of a vector-controlled PMSG-based WECS and its

correlation with key control variables. The top plot shows the rotor speed, which starts from zero and increases smoothly, following a stepped reference trajectory. The presence of a closely overlapping red line indicates that the system tracks the reference speed, which is likely determined by the MPPT algorithm. At specific time instances, around 0.8s and 1.2s, the speed undergoes slight reductions, reflecting system responses to changing wind conditions or control actions. The middle plot represents the q-axis current, which is directly responsible for torque generation in the PMSG. As the speed increased, quadrature current became more negative, signifying an increase in the generator torque to achieve the required acceleration.

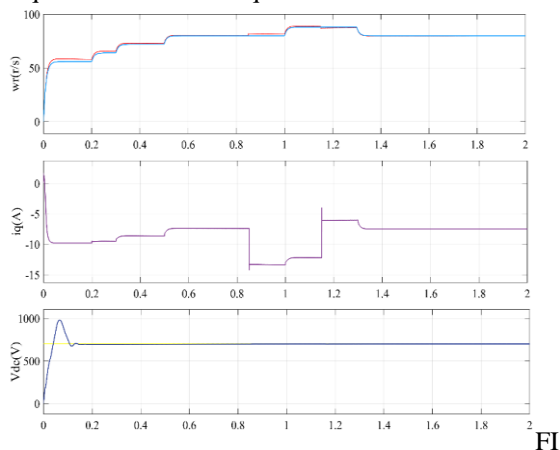


FIGURE 6 Speed Response Analysis Under Different Control Variants.

At the speed transition points, exhibits transient fluctuations, highlighting its role in adjusting the torque to maintain an accurate speed tracking. The lower plot illustrates the DC link voltage, which initially exhibited a significant peak due to startup transients before settling at around 700V. The stability of DC link voltage, despite variations in speed and quadrature current, confirms the effectiveness of the power electronic converters in regulating energy flow. The close tracking of the rotor speed to its reference, along with quadrature current adjustments and a well-regulated DC voltage, demonstrates the efficiency of the vector control strategy in ensuring smooth and stable operation of the PMSG-WECS.

3.2 Simulation result of reference current generation using the DTOGI Algorithm.

Figure 7 illustrates an innovative approach to reference current generation to compensate for nonlinear load effects, which is a critical aspect of power-quality enhancement in grid-connected systems. The nonlinear load introduces harmonic-rich pulsating currents that require precise reference-current extraction to mitigate power distortions and enhance system stability. Initially, the nonlinear load current exhibited high-frequency oscillations owing to switching components. The second and third waveforms depict the transformation of this distorted current into (alpha-beta) reference frame components simplifying the decomposition of the fundamental and harmonic elements. This transformation is pivotal for the implementation of advanced power-compensation control strategies. Unlike conventional filtering techniques, DTOGI offers superior selectivity and rapid adaptation to dynamic load variations, making it highly effective in distinguishing between fundamental and harmonic components. The next set of current waveforms shows the precise identification of harmonic distortions in the dq reference frame, ensuring the accurate compensation of non-active power components. The unit voltage components were then synthesized to regulate the compensating current, providing an optimal response for load variations. Finally, the reference current derived from this multistage transformation process guides the inverter to generate a compensating current that actively cancels harmonics and reactive power, resulting in a near-ideal sinusoidal grid current. This is a necessary development in modern active power filtering and renewable energy grid integration since it guarantees greater power quality, lower THD, and better grid voltage stability.

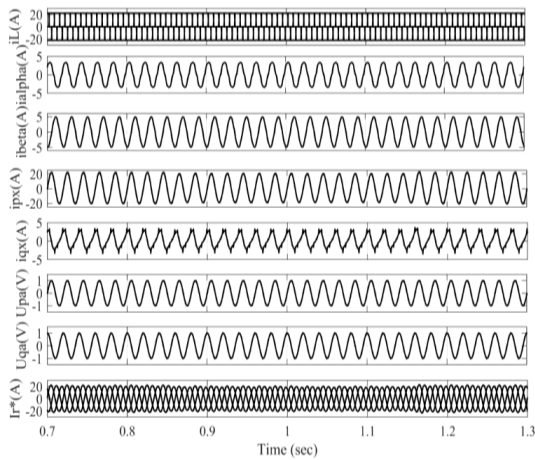


FIGURE 7: Simulation Outcome for Reference Current Generation

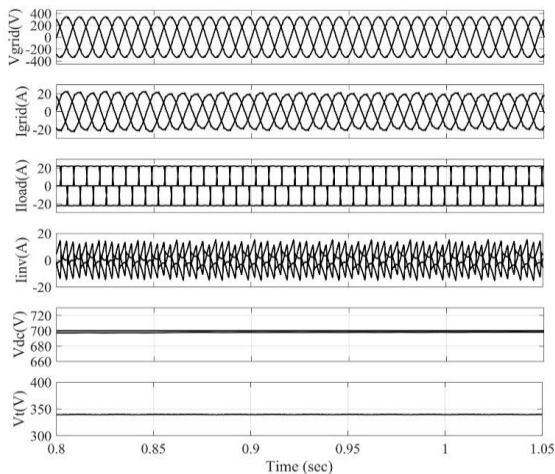


FIGURE 8: Simulation Outcome of Grid-Side DTOGI Control Performance

Figure-8 shows, using a DTOGI current-control loop, the grid-side performance of a PMSG-based WECS controlled. The grid voltage stayed just sinusoidal, suggesting effective grid synchronization free of any obvious distortion. Furthermore, sinusoidal and in phase with the voltage, the grid current promises effective power injection with little harmonic distortion, hence improving the power quality. The current load exhibits a square waveform, suggesting a nonlinear or pulsating load demand. However, the inverter current displays a high-frequency switching pattern, which is characteristic of hysteresis pulse-width modulation control, demonstrating the inverter's capability to compensate for the nonlinear load while maintaining a clean sinusoidal grid current. The DC-link voltage

remains stable at approximately 700V, with minimal fluctuations, confirming the effectiveness of the DTOGI-based control strategy in regulating the DC bus voltage and ensuring steady power conversion from the wind turbine to the grid. Similarly, the terminal voltage remained nearly constant at approximately 350V, validating the ability of the DTOGI control to stabilize the system voltage despite variations in the load and inverter operation. These attributes are essential for efficiently integrating wind energy into the grid, reducing harmonics, and maintaining smooth operation under varying load conditions.

3.3 Simulation Performance of Fixed wind speed under Load Variation

Based probably on a PMSG, the figure-9 shows the dynamic activities of a grid-connected WECS. Under different load conditions, the provided waveform shows the execution of the DTOGI control method in preserving the stability of grid voltage, DC voltage, and frequency. The primary object of this study is to evaluate the control strategy's ability to sustain system stability when the load varies within the range of 0.7 to 1.1 second. The waveform illustrates that the grid voltage remained stable despite changes in the load. No significant deviations, distortions, or excessive fluctuations are observed. The voltage waveform retains its sinusoidal nature, indicating that the DTOGI controller effectively mitigates the disturbances. The DC-link voltage shows minimal fluctuations during load variations, which confirms the effectiveness of the controller in regulating the DC bus voltage. A stable DC voltage is critical for ensuring smooth power conversion and maintaining the reliability of the system. Frequency stability waveform analysis also confirmed that the grid frequency remained within acceptable limits throughout the load variation range. Frequency stability is crucial for synchronizing renewable energy sources with the grid and ensuring continuous and stable power delivery.

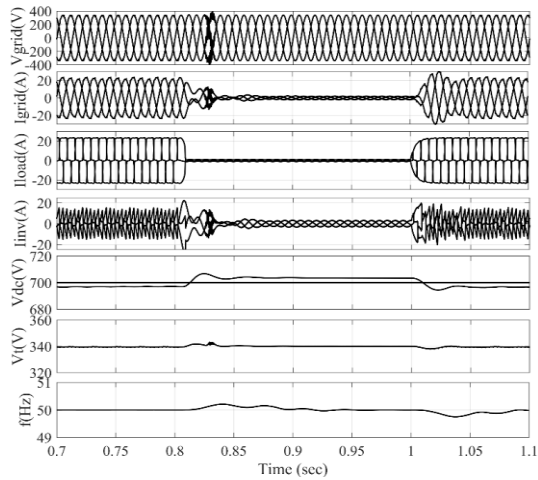


FIGURE 9. Impact of Sudden Load Variation at PCC: Simulation Results

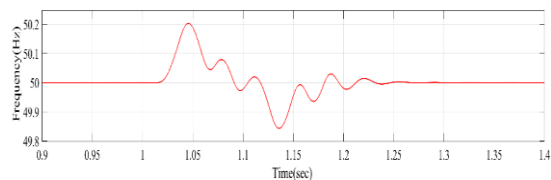


FIGURE 10 Grid Frequency Behaviours During a Transient Disturbance

The stability of the waveform shown in figure 10 indicates that grid synchronization is well maintained. The grid voltage angle progresses consistently without significant disturbances, meaning that the phase-locked loop (DFOGI-PLL) is correctly used for synchronization functions. The frequency remains steady with only small variations, suggesting that the wind generation system and its control strategies effectively regulate power exchange with the grid. The fluctuations observed in other waveforms (such as the grid current and load current) do not significantly affect the grid voltage angle or frequency, implying that the system is robust against transient disturbances. The results validate that the proposed control approach effectively suppresses disturbances and enhances system robustness. This makes it a viable alternative for enhancing the performance of PMSG-based wind energy systems and facilitating smooth grid connection.

3.4 Power Quality analysis under Steady-State Conditions

Figure 11 shows the outcomes of a steady

condition's simulation study of the power-quality parameters. Despite the considerable distortion in the load current, the data clearly shows that the THD in both the grid current and the load current stays within the designated limit of five percent, as advised by many criteria. With respective values of 1.70%, 2.86%, and 26.27%, the grid voltage, grid current, and load current displayed distortions with magnitudes respectively.

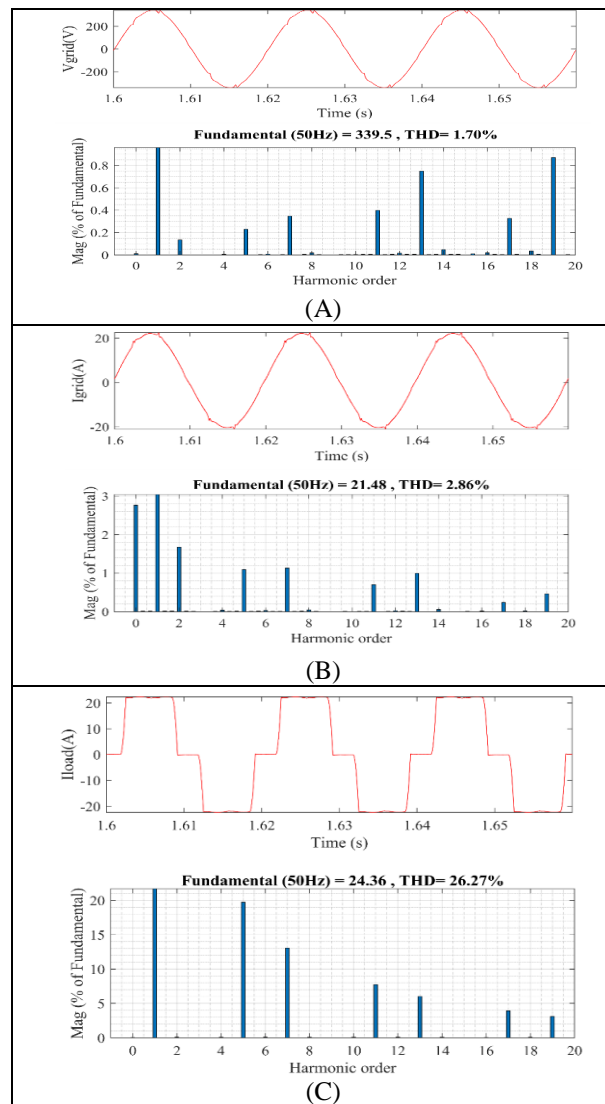


FIGURE 11 Waveform Distortion Expressed as Percentage THD (A) Phase A Grid Voltage (B) Phase A Grid Current (C) Phase A Load Current

3.5 Comparison of NLMS, SOSF and DFOGI control

Figure 12 presents the DC link voltage control parameters, which provides a comparison of the

various control techniques. The effectiveness of each approach in maintaining stable and efficient voltage regulation under dynamic conditions was evaluated through crucial parameters, including transient parameters such as rise time, settling time, peak time, and overshoot. The stability parameters of the DC-link voltage representing the NLMS SOSF and DTOGI control algorithms are listed in Table 6.2. This tabulation provides a detailed comparison of the essential performance metrics, encompassing all stability parameters.

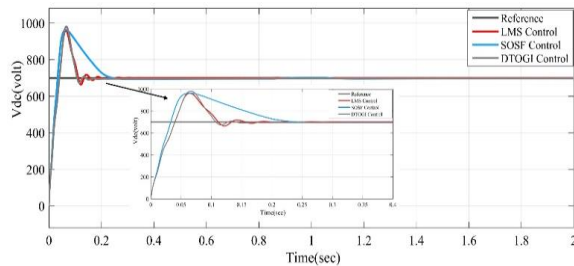


FIGURE-12 Comparison of DC Link Voltage Behaviours Under Transient Conditions

The results show that in control of the DC-link voltage for grid-connected PMSG systems, the DTOGI control algorithm beats alternative techniques. Its enhanced dynamic response and stability, characterized by reduced overshoot and quicker settling time, make it particularly well suited for applications involving fluctuating operating conditions. This superior performance establishes the DTOGI control algorithm as a more efficient approach for managing voltage in these systems.

TABLE 2: Stability Parameter Analysis of DC Link Voltage

Sr No	Control Parameter	NLMS Control Algorithm	SOSF Control Algorithm	DTOGI Control Algorithm
1	Rise time	0.02 to 0.04 sec	0.025 to 0.05 sec	0.018 to 0.03 sec
2	Peak time	0.065 sec	0.07 sec	0.06 sec
3	Transient overshoot	32.86 %	40 %	28 %
4	Delay time	0.015 sec	0.017 sec	0.012 sec
5	Settling time	0.22 sec	0.3 sec	0.2 sec

In this study, we analysed the performance of three different control algorithms, NLMS, SOSF, and DTOGI, in regulating the DC link voltage stability. Examined are key performance measures including rising time, peak time, transient peak overshoot, delay time, and settling time.

TABLE 3: Analysis of Stability Parameters in DC Link Voltage Regulation

Sr No	Control Parameter	Key Point
1	Rise time	1)DTOGI achieves the fastest rise time (0.018 to 0.03 sec), meaning it responds more quickly than NLMS (0.02 to 0.04 sec) and SOSF (0.025 to 0.05 sec). 2)A shorter rise time is advantageous since it facilitates a rapid response to alterations in system circumstances, hence diminishing the likelihood of extended instability.
2	Peak time	1)DTOGI exhibits the shortest peak time (0.06 sec), which is lower than NLMS (0.065 sec) and SOSF (0.07 sec). 2)A lower peak time implies a faster voltage regulation process, reducing the duration of transient disturbances.
3	Transient Peak overshoot	1)DTOGI has the lowest overshoot (28%) compared to NLMS (32.86%) and SOSF (40%). 2)A lower overshoot is beneficial because it minimizes excessive voltage spikes that could lead to stress on power electronic components, improving system reliability.
4	Delay time	1)DTOGI exhibits the shortest delay time (0.012 sec), outperforming NLMS (0.015 sec) and SOSF (0.017 sec). 2)A lower delay time indicates a more responsive system, reducing latency in voltage correction.
5	Settling time	1)DTOGI achieves the fastest settling time (0.2 sec), compared to NLMS (0.22 sec) and SOSF (0.3 sec). 2)A shorter settling time is highly desirable because it ensures that the system reaches a stable operating condition quickly, improving overall system efficiency.

IV. APPENDIX

PMSG(Cylindrical Type Rotor)	3.7 KW,10A,50 Hz, 240 V(L-L)
Te(Maximum Torque)	47 Nm
W(Rated Speed)	60 rad/sec
p (Number of a pole)	8
p_n (Pole Pair)	4
Rs(Resistance of stator)	4.2 ohm
Lq & Ld(Quadrature axis inductance & Direct axis inductance)	8.5 mH
λ_m (flux of permanent magnets)	0.498 Wb
Grid Specification	3-phase, 415 V (L-L), 50 Hz
Non-linear Load	$R = 25 \Omega$, $L = 100 \text{ mH}$
Control Parameter of DTOGI Control	$V_{DC} = 700 \text{ V}$, $K_o = 0.2$ and $K_1 = \sqrt{2}$
DC Capacitance	$C_{dc} = 8000 \mu\text{F}$
Inverter inductor interface	$L_f = 5 \text{ mH}$
Grid filter	$R_f = 5 \Omega$, $C_f = 10 \mu\text{F}$

V. CONCLUSIONS

An analysis was conducted on a three-phase PMSG-based grid-connected system with improved power quality. For grid-connected operations, vector control facilitates synchronization of the PMSG output with the grid frequency while ensuring a rapid response to disturbances. This study evaluated the use of the DTOGI current control approach in a wind energy system under random input variations, demonstrating a significantly improved rate of convergence. This control strategy proved to be effective for both balanced and unbalanced load conditions. The DTOGI algorithm plays a vital role in regulating the DC-link voltage and preserving power balance between the source and output. A comparative investigation of several control approaches indicates that DTOGI attains a DC-link voltage settling time of 0.2 seconds, with an acceptable voltage variation of around 0.65 volts. After the load variation, the system parameters instantly returned to their original values, ensuring stability and reliability. Additionally, the proposed approach mitigates harmonic effects, reducing the

THD to below 5% in compliance with the standards.

Future work will aim to further enhance the adaptive DTOGI control technique by incorporating advanced fault detection and mitigation strategies, optimizing the control algorithm for real-time applications, and assessing its scalability to larger grid-connected systems. Additionally, this study explores its performance under varying environmental conditions and its interaction with smart grid technologies.

REFERENCES

- [1]. T. Y. Heng, T. J. Ding, C. C. W. Chang, T. J. Ping, H. C. Yian, and M. Dahari, "Permanent magnet synchronous generator design optimization for wind energy conversion system: A review," *Energy Reports*, vol. 8, pp. 277–282, 2022. doi:10.1016/j.egy.2022.10.239.
- [2]. H. Shutari, T. Ibrahim, N. B. M. Nor, Y. Z. Alharthi, and H. Abdulrab, "Control approaches of power electronic converter interfacing grid-tied PMSG-VSWT system: A comprehensive review," *Heliyon*, vol. 10, no. 12, e32032, 2024. doi:10.1016/j.heliyon.2024.e32032.
- [3]. M. Hosny, M. I. Marei, and A. M. I. Mohamad, "Adaptive hybrid virtual inertia controller for PMSG-based wind turbine based on fuzzy logic control," *Scientific Reports*, vol. 15, no. 1, p. 3757, 2025. doi:10.1038/s41598-025-87986-6.
- [4]. A. Fathelkhair, H. Abouobaida, Y. Mchaouar, Y. Abouelmahjoub, K. Oualifi, and J. M. Guerrero, "Sensorless nonlinear control of permanent magnet synchronous generator based wind energy conversion systems," *Electrical Engineering*, 2025. doi:10.1007/s00202-025-03008-8.
- [5]. Devashish, A. Thakur, S. Panigrahi, and R. R. Behera, "A review on wind energy conversion system and enabling technology," in *Proc. Int. Conf. Electrical Power and Energy Systems (ICEPES)*, pp. 527–532, 2016. doi:10.1109/ICEPES.2016.7915985.
- [6]. H. S. Kim and D. D.-C. Lu, "Wind energy conversion system from electrical perspective—A survey," *Smart Grid and*

- Renewable Energy*, vol. 1, no. 3, pp. 119–131, 2010. doi:10.4236/sgre.2010.13017.
- [7]. J. Li, G. Wang, Z. Li, S. Yang, W. T. Chong, and X. Xiang, "A review on development of offshore wind energy conversion system," *Int. J. Energy Research*, vol. 44, no. 12, pp. 9283–9297, 2020. doi:10.1002/er.5751.
- [8]. S. Manna, D. K. Singh, and A. K. Akella, "A review of control techniques for wind energy conversion system," *Int. J. Eng. Technol. Innovation*, vol. 13, no. 1, pp. 40–69, 2023. doi:10.46604/ijeti.2023.9051.
- [9]. Y. Errami, M. Ouassaid, and M. Maaroufi, "Control of a PMSG-based wind energy generation system for power maximization and grid fault conditions," *Energy Procedia*, vol. 42, pp. 220–229, 2013. doi:10.1016/j.egypro.2013.11.022.
- [10]. J. Wang, D. Xu, B. Wu, and Z. Luo, "A low-cost rectifier topology for variable-speed high-power PMSG wind turbines," *IEEE Trans. Power Electron.*, vol. 26, no. 8, pp. 2192–2200, 2011. doi:10.1109/TPEL.2011.2106143.
- [11]. M. Aoumri, A. Harrouz, I. Yaichi, S. Baala, and P. Wira, "Robustness investigation of FOC of PMSG based variable-speed wind turbine connected on grid," in *Proc. 3rd Int. Conf. Advanced Electrical Engineering (ICAEE)*, pp. 1–5, 2024. doi:10.1109/ICAEE61760.2024.10783398.
- [12]. S. M. Tripathi, A. N. Tiwari, and D. Singh, "Optimum design of proportional-integral controllers in grid-integrated PMSG-based wind energy conversion system," *Int. Trans. Electr. Energy Syst.*, vol. 26, no. 5, pp. 1006–1031, 2016. doi:10.1002/etep.2120.
- [13]. F. Blaabjerg, R. Teodorescu, M. Liserre, and A. V. Timbus, "Overview of control and grid synchronization for distributed power generation systems," *IEEE Trans. Ind. Electron.*, vol. 53, no. 5, pp. 1398–1409, 2006. doi:10.1109/TIE.2006.881997.
- [14]. J. Li-Jun et al., "Unbalanced control of grid-side converter based on DSOGI-PLL," in *Proc. IEEE 10th Conf. Industrial Electronics and Applications (ICIEA)*, pp. 1145–1149, 2015. doi:10.1109/ICIEA.2015.7334279.
- [15]. L. Peng, Z. Fu, T. Xiao, Y. Qian, W. Zhao, and C. Zhang, "An improved dual second-order generalized integrator phased-locked loop strategy for an inverter of flexible high-voltage direct current transmission systems under nonideal grid conditions," *Processes*, vol. 11, no. 9, p. 2634, 2023. doi:10.3390/pr11092634.
- [16]. P. Bansal, S. Dixit, S. Gupta, M. A. Alotaibi, H. Malik, and F. P. García Márquez, "A robust modified notch filter-based SOGI-PLL approach to control multilevel inverter under distorted grid," *Ain Shams Eng. J.*, vol. 15, no. 5, p. 102675, 2024. doi:10.1016/j.asej.2024.102675.
- [17]. A. Ranjan, S. Kewat, and B. Singh, "DSOGI-PLL with in-loop filter-based solar grid interfaced system for alleviating power quality problems," *IEEE Trans. Ind. Appl.*, vol. 57, no. 1, pp. 730–740, 2021. doi:10.1109/TIA.2020.3029125.
- [18]. S. Prakash, J. K. Singh, R. K. Behera, and A. Mondal, "A Type-3 modified SOGI-PLL with grid disturbance rejection capability for single-phase grid-tied converters," *IEEE Trans. Ind. Appl.*, vol. 57, no. 4, pp. 4242–4252, 2021. doi:10.1109/TIA.2021.3079122.
- [19]. B. Liu et al., "A simple approach to reject DC offset for single-phase synchronous reference frame PLL in grid-tied converters," *IEEE Access*, vol. 8, pp. 112297–112308, 2020. doi:10.1109/ACCESS.2020.3003009.
- [20]. J. Yu, Y. Xu, Y. Cao, and J. Yu, "An improved dual second-order generalized integrator PLL under non-ideal grid conditions," in *Proc. 35th Chinese Control Conf. (CCC)*, pp. 8644–8648, 2016. doi:10.1109/ChiCC.2016.7554736.
- [21]. S. Golestan, E. Ebrahimzadeh, B. Wen, J. M. Guerrero, and J. C. Vasquez, "dq-frame impedance modelling of three-phase grid-tied voltage source converters equipped with advanced PLLs," *IEEE Trans. Power Electron.*, vol. 36, no. 3, pp. 3524–3539, 2021. doi:10.1109/TPEL.2020.3017387.
- [22]. S. Golestan, J. M. Guerrero, and J. C. Vasquez, "Steady-state linear Kalman filter-based PLLs for power applications: A second look," *IEEE Trans. Ind. Electron.*, vol. 65, no. 12, pp. 9795–9800, 2018. doi:10.1109/TIE.2018.2823668.
- [23]. M. Singh and A. Chandra, "Power maximization and voltage sag/swell ride-

through capability of PMSG-based variable speed wind energy conversion system," in *Proc. IECON Industrial Electronics Conf.*, pp. 2206–2211, 2008.

Author details

1)Mr. Devang B Parmar:-

(Ph.D Scholar,Gujarat Technological University,Ahmedabad-382424, Gujarat, India)

Mr. Devang B. Parmar has the position of Assistant Professor at VVP Engineering College, Rajkot. He obtained his master's degree from Gujarat Technological University in 2012 and is currently pursuing a Ph.D. at the Gujarat Technological University institution. His research interests encompass PMSG converter topologies for wind-based power generation systems, high-voltage engineering, control systems, and power electronics applications in distributed power generation systems.

2)Dr. Ashutosh K. Giri

(Government Engineering College Bharuch-392002, Gujarat, India)

Dr. Ashutosh K. Giri serves as an Assistant Professor at the Government Engineering College, Bharuch. He obtained his Ph.D. in Electrical Engineering from the Sardar Vallabhbhai National Institute of Technology, Surat, India, during the period from 2016 to 2020. His primary area of interest and specialization lies in Power Electronics Applications within Distributed Power Generation Systems. His research interests encompass the study of single-phase induction generators, three-phase self-excited induction generators, and permanent magnet synchronous generators, with a focus on novel converter topologies for wind-based power generation systems. Additionally, he investigates power quality issues in distributed power generation systems and the design and implementation of adaptive control algorithms for D-STATCOM utilized in non-conventional energy sources.